Iron−Ligand Structure and Iron Redox Property of Nitric Oxide Reductase Cytochrome P450nor from *Fusarium oxysporum*: Relevance to Its NO Reduction Activity†

Yoshitsugu Shiro,* Motoyasu Fujii,‡ Yasuhiro Isogai, Shin-ichi Adachi, and Tetsutaro Iizuka

The Institute of Physical and Chemical Research (RIKEN), Wako, Saitama 351-01, Japan

Eiji Obayashi

Department of Applied Chemistry, Chuo University, Bunkyo-ku, Tokyo 112, Japan

Ryu Makino

Molecular Biochemistry I, Faculty of Science, Himeji Institute of Technology, Akou-gun, Hyougo 678-12, Japan

Kazuhiko Nakahara and Hirofumi Shoun

Institute of Applied Biochemistry, University of Tsukuba, Tsukuba, Ibaraki 305, Japan

Received January 17, 1995; Revised Manuscript Received March 27, 1995®

ABSTRACT: We studied the nitric oxide reductase, cytochrome P450nor, purified from a denitrifying fungus *Fusarium oxysporum* with electron paramagnetic resonance spectral and redox potential measurements. The EPR spectral features of P450nor in the ferric resting, the ferric cyanide-bound, and the ferrous NO-bound forms were the same as the corresponding ones of other general P450s such as *Pseudomonas putida* P450cam. In contrast, the metyrapone complex of ferric P450nor gave an EPR spectrum with significantly different *g* values from that of P450cam. The EPR results were explained in terms of similarity in the immediate configuration of the S^-−Fe−ligand (H_2O, CN^-, NO) structure between P450nor and P450cam but a structural difference at the heme distal pocket, especially in the substrate binding domain; P450cam has a camphor binding domain, while P450nor does not. In spite of the same S^-−Fe−H_2O configuration, the redox potential of P450nor in the ferric/ferrous couple was measured to be −307 mV, which is much lower than those of the camphor-bound (−140 mV) and -free (−250 mV) P450cam. The lower redox potential could be attributable to the different electrostatic interaction of the heme with its surroundings; e.g., the heme environment of P450nor is charged either more negatively or less positively than P450cam. The low redox potential of P450nor is favorable for the reductive activation of the NO ligand, in good consistency with its reaction mechanism which we have proposed [Shiro et al. (1995) *J. Biol. Chem.* (in press)], where the NO ligand bound to the ferric iron is reduced with two electrons from NADH and then reacts with another NO, yielding N_2O and H_2O. The EPR and redox data were also discussed in relation to the unique properties of P450nor.

Denitrification is an important process in the global nitrogen cycle, in which NO_3^- and/or NO_2^- is reduced to gaseous forms of nitrogen compounds, either N_2 or N_2O. A large number of bacteria (prokaryotes) perform this process, which consists of some consecutive chemical reactions catalyzed by metalloenzymes. In the denitrifying process, a controversy surrounded the question of whether NO is the chemical intermediate prior to N_2O, the first recognized species with N,N-bond antecedents to N_2. Recently, enzymes with NO reduction activity, NOR,[1] were isolated from *Pseudomonas stutzeri* and *Paracoccus denitrificans*, providing evidence for the principal denitrification pathway of $NO_2^- \rightarrow NO \rightarrow N_2O$, with NO being a free and obligatory intermediate, and N,N-bond formation catalyzed by NOR (Carr & Ferguson, 1990; Carr et al., 1989; Dermastia et al., 1991; Goretski & Hollocher, 1990; Heiss et al., 1989; Kastrau et al., 1994; Turk & Hollocher, 1992).

The NORs from *P. stutzeri* and from *Pa. denitrificans* are complexes of two membrane-bound hemoproteins, cytochrome *bc* complex, having apparent molecular masses of ~37−38 kDa (cytochrome *b*) and ~17−18 kDa (cytochrome *c*). Zumft and his co-workers have studied the molecular properties of NOR from *P. stutzeri* with biochemical and spectroscopic methods (Kastrau et al., 1994; Zumft, 1993). Its EPR spectrum in the ferric state exhibits some complexity, in which the high spin component ($g = 6$) coming from the five-coordinate cytochrome *b* together with the low spin component (around $g = 2$) from the six-coordinate cyto-

† This work was supported by Biodesign Research Program from RIKEN, by the MR Science Research Program in RIKEN, and by Special Coordination Funds from the Science and Technology Agency of Japan.

* To whom correspondence should be addressed.

‡ Present address: Department of Biophysical Engineering, Faculty of Engineering Science, Osaka University, Toyonaka, Osaka 560, Japan.

® Abstract published in *Advance ACS Abstracts,* June 15, 1995.

[1] Abbreviations: NOR, nitric oxide reductase; EPR, electron paramagnetic resonance; P450nor, cytochrome P450 from *Fusarium oxysporum*; P450cam(+), *d*-camphor-bound form of cytochrome P450 from *Pseudomonas putida*; P450cam(−), *d*-camphor-free form of cytochrome P450 from *Pseudomonas putida*.

0006-2960/95/0434-9052$09.00/0

chrome *c* is observed. Further, they measured their redox potentials to be +322 mV for cytochrome *b* and +280 mV for cytochrome *c*. On the basis of these results, several mechanisms for the NO reduction catalyzed by NOR have been proposed and discussed (Ye et al., 1994; Dermastia et al., 1991; Turk & Hollocher, 1992).

Most recently, Shoun and his co-workers (Shoun et al., 1989; Shoun & Tanimoto, 1991) found that a fungus *Fusarium oxysporum* exhibits a distinct denitrifying ability which results in the anaerobic evolution of N_2O from NO_3^- and NO_2^-. This was a first report of the denitrification by a eukaryote. Further, they purified an NOR from *F. oxysporum* grown in the presence of NO_3^-/NO_2^- and identified it as a kind of a heme–enzyme cytochrome P450 on the basis of its CO difference spectrum (λ_{max} = 447 nm) (Nakahara et al., 1993, 1994). As identified by its name, cytochrome P450nor, it can be classified into the P450 superfamily on the basis of its cDNA analysis (Kizawa et al., 1991; Obika et al., 1993). The enzyme showed at most a 40% identity in the primary structure to some bacterial P450s.

In spite of these similarities, the functional property of P450nor is so unique that it exhibits NO reduction activity, but not monooxygenation activity. This is sharply contrasted with the general P450s, which catalyze the monooxygenation reaction; i.e., an oxygen atom from O_2 is inserted into an organic substrate. The NO reduction reaction catalyzed by P450nor was established as follows:

$$2NO + NADH + H^+ \rightarrow N_2O + NAD^+ + H_2O$$

Corresponding to the lack of monooxygenation activity, the O_2 complex of P450nor is too unstable to be spectroscopically detected even at −20 °C.[2] These observations allow us to suggest that the structure of P450nor in the heme environment may be somewhat different from that of the general P450s.

In our previous work, we carried out kinetic and thermodynamic studies of the CO binding to P450nor and showed that the channel for the external ligand to have access to the heme iron is opened more widely in P450nor than that in P450cam (Shiro et al., 1994). Further, on the basis of the kinetic analysis of the reaction of the enzyme with NO and NADH, we proposed the molecular mechansim of the catalytic reaction in the NO reduction to N_2O (Shiro et al., 1995). However, we have not yet obtained any information on the immediate structure of the heme iron and its redox property. Therefore, in the present study, we investigated the EPR spectral and the redox potential measurements of P450nor to characterize the iron–ligand structure and the heme–protein interaction. The results obtained are discussed with relevance to the unique functional properties of P450nor and its reaction mechanism in the NO reduction we have proposed. Further, we also compare the molecular properties of P450nor with those of the bacterial NOR from *P. stutzeri*.

MATERIALS AND METHODS

Enzyme. Cytochrome P450nor was isolated from *F. oxysporum* and purified according to the methods described previously (Shoun et al., 1983; Nakahara et al., 1993). The enzyme was dissolved in 0.1 M potassium phosphate buffer, pH 7.2, and was concentrated to about 1.2 mM with a DIAFLO membrane (Amicon). The concentrated enzyme solution was diluted with the buffer to ~0.1 mM for the EPR measurement and to ~10 μM for the redox potential measurement.

EPR Measurement. The EPR spectra were measured with a JEOL JES-RE 1X spectrometer equipped with an Air Products Model LTR-3 Heli-tran cryostat system, in which the temperature was monitored with a Scientific Instruments Series 5500 temperature indicator/controller.

Redox Potential Measurement. The oxidation–reduction potential for the ferric/ferrous couple of P450nor was monitored by a combined platinum microelectrode (Ingold, Pt 4800). The electrode was connected to a Corning pH–mV meter, Model 125. The mediator used was a mixture of α-hydroxyphenazine, phenosafranine, safranine T, and benzyl viologen. The ferric P450nor was photoreduced in the presence of 50 mM EDTA and 1 mM proflavine sulfate in 0.1 M potassium phosphate buffer at 20 °C. The spectral change in the photoreduction was monitored with a Shimadzu MPS 2000 spectrophotometer. Details were described elsewhere (Makino et al., 1982; Shiro et al., 1993).

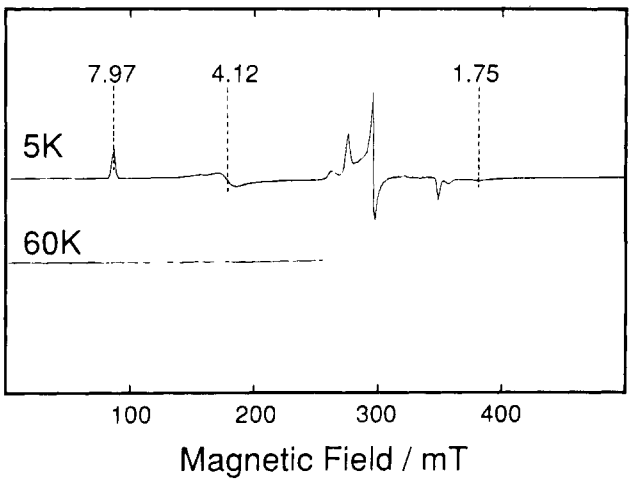

FIGURE 1: EPR spectra of cytochrome P450nor in the ferric resting state at 5 and 60 K.

RESULTS

EPR Measurement of Ferric Resting State. Figure 1 shows the EPR spectrum of P450nor in the ferric resting state at 5 K. In this spectrum, two sets of EPR signals are observed: the signals from the ferric high spin (H.S.) component (g_x = 7.97, g_y = 4.12, g_z = 1.75) and from the low spin (L.S.) one (g_z = 2.442, g_y = 2.260, g_x = 1.911). The H.S. signals were not detectable at 60 K, due to fast electron-spin relaxation. The spectral characteristics are basically the same as those of other usual P450s, such as P450cam, as is compared in Table 1, although the proportion of the H.S. component relative to the L.S. one is smaller, compared with that of P450cam(+) (Lipscomb, 1980; Dawson et al., 1982). Correspondingly, the optical absorption spectrum of P450nor at 77 K predominantly exhibited the ferric L.S. feature (data not shown).

In Figure 2A, the L.S. region around $g \sim 2$ is expanded. In addition to a set of the major L.S. signals (*vide supra*), minor signals are observed at g_z = 2.543, g_y = 2.24, and g_x = 1.870. The *g*-values are comparable to those of the

[2] M. Fujii and Y. Shiro, unpublished results.

Table 1: Comparison of EPR Parameters between Cytochromes P450nor and P450cam

complexes	g values			coupling const	ref
Fe^{3+}(H.S.)	g_x	g_y	g_z		
P450nor	7.97	4.12	1.75		this work
P450cam(+)	7.85	3.97	1.78		*a*
Fe^{3+}(L.S.)	g_z	g_y	g_x		
P450nor	2.442	2.260	1.911		this work
P450cam(+)	2.42	2.24	1.97		*a*
P450cam(−)	2.45	2.26	1.91		*a*
Δ_1	−0.02	−0.02	0.06		*b*
Δ_2	0.01	0.00	0.00		*c*
$Fe^{3+}CN^-$	g_z	g_y	g_x		
P450nor	2.592	2.307	1.821		this work
P450cam	2.60	2.28	1.82		*a*
Δ	0.01	−0.03	0.00		*d*
Fe^{3+}metyrapone	g_z	g_y	g_x		
P450nor	2.561	2.264	1.846		this work
P450cam	2.47	2.27	1.92		*e*
Δ	−0.09	0.01	0.07		*d*
Fe^{2+}NO(P450 type)	g_x	g_z	g_y	A_z (mT)	
P450nor	2.082	2.007	1.97	2.00	this work
P450cam(±)	2.073	2.009	1.976	1.92	*f*
Δ	−0.009	0.002	0.01		*d*
Fe^{2+}NO(P420 type)	g_x	g_z	g_y	A_z (mT)	
P450nor	2.110	2.012		1.72	this work
P450cam(±)	2.072	2.015		1.6	*f*
Δ	−0.038	0.003			*d*

[a] Lipscomb (1980). [b] $\Delta_1 = g$(P450cam(+)) − g(P450nor). [c] $\Delta_2 = g$(P450cam(−)) − g(P450nor). [d] $\Delta = g$(P450cam) − g(P450nor). [e] Peterson et al. (1971). [f] O'Keeffe et al. (1978).

imidazole complex of ferric P450cam ($g_z = 2.56$, $g_y = 2.27$, $g_x = 1.87$) (Lipscomb, 1980), suggesting the coordination of the nitrogenous ligand to the ferric iron at its sixth site. Although we cannot identify the minor component in more detail at the present stage, the same feature was also observed in the EPR spectrum of P450cam.

EPR Measurements of Ferric Cyanide and Metyrapone Complexes. In the EPR spectrum of the cyanide complex of ferric P450nor, two sets of signals were observed (data not shown). A similar observation was previously reported for the ferric CN^- complex of P450cam by Lipscomb (1980), where more than one L.S. species was observed, possibly due to either a different binding geometry of the CN^- ligation or binding of both protonated and unprotonated species. However, for the CN^- complex of P450nor, addition of glycerol (finally 10%) resulted in one set of the low spin signals (Figure 2B). As compared in Table 1, the g-values of the resultant spectrum are the same as those reported for the P450cam cyanide complex (Lipscomb, 1980).

In Figure 2C is illustrated the EPR spectrum of the metyrapone complex of ferric P450nor, in which only one set of absorptions is unambiguously observed. Comparing the g-values with those of the P450cam metyrapone complex (Peterson et al., 1971), the differences in the g_x and g_z values (Δg_x and Δg_z) are 0.09 and −0.07, respectively (Table 1). The magnitude of the difference is significantly larger than those for other derivatives between P450nor and P450cam, which are at most 0.02. This difference probably arises from the different structural and/or electronic interaction of the heme and the ligand, which will be discussed in the Discussion section.

EPR Measurements of Ferrous Nitric Oxide Complex. We tried to measure the EPR spectrum of the NO complex of

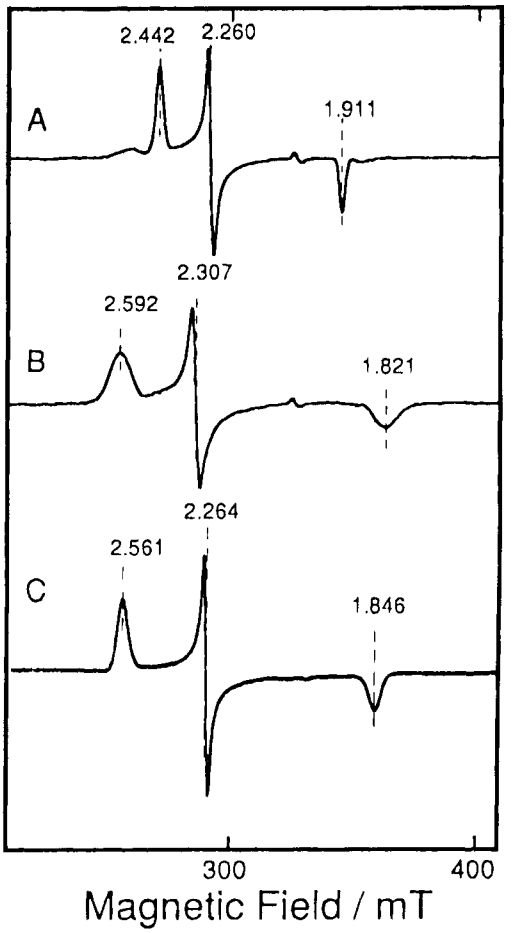

FIGURE 2: EPR spectra of the ferric low spin complexes of cytochrome P450nor at 35 K. (A) is the spectrum of the ferric resting enzyme, which was dissolved in 0.1 M phosphate buffer at pH 7.2. As was measured in 0.1 M HEPES buffer, the minor components increased in their signal intensities. (B) is the spectrum of the cyanide complex, which is dissolved in 0.1 M phosphate buffer containing 10% glycerol. The cyanide concentration is about 10 mM. (C) is the spectrum of the metyrapone complex. This species gave the same spectrum independently of the buffer condition.

ferrous P450nor, which was prepared by reduction of the ferric enzyme with $Na_2S_2O_4$ in the presence of $NaNO_2$ under a N_2 atmosphere. Immediately (about 1 min) after the preparation, we froze the sample solution in liquid N_2 (77 K) and measured its EPR spectrum at 35 K. The spectrum for the sample prepared in this manner shows some complexity, as shown in Figure 3A. We then measured the spectrum of the sample which was frozen about 5 min after the preparation (Figure 3B). On comparing these two spectra (Figure 3A,B), it was found that the spectrum changed with the passage of time; for example, the signal at $g_x = 2.082$ decreased in its intensity with a concomitant increase in the intensity of the signal at $g_x = 2.11$. The result indicated that, in the P450nor NO derivative, one species (**X**) gradually converted into another species (**Y**).

We then calculated the difference spectra from these two spectra, denoted by **A** for Figure 3A and **B** for Figure 3B, to obtain the pure spectra of **X** and **Y**. First, we obtained the spectrum of **X** according to the equation, $\mathbf{X} = \mathbf{A} - k\mathbf{B}$, where the k value (0.85) was set to eliminate the signal at $g = 2.11$ in the spectrum of **X**. Similarly, we obtained the spectrum of **Y** from $\mathbf{Y} = \mathbf{B} - k'\mathbf{A}$, in which the k' value (0.36) was set to eliminate the signal at $g = 2.082$. The

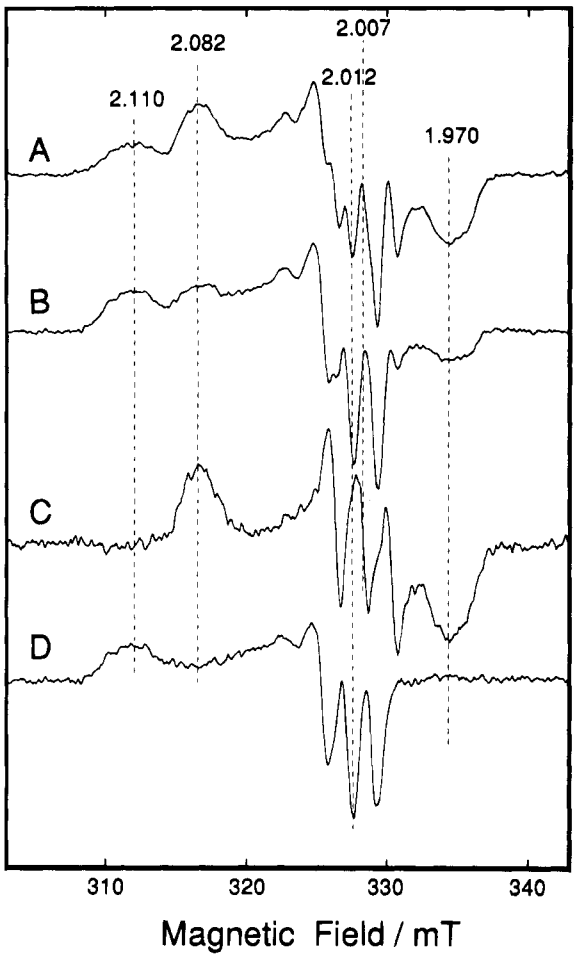

FIGURE 3: EPR spectra of cytochrome P450nor prepared on the reaction with $NaNO_2$ and $Na_2S_2O_4$. (A) The spectrum taken at 1 min after the sample preparation, and (B) that at 5 min after the preparation. (C) and (D) The difference spectra calculated from those of (A) and (B). The method to calculate these spectra are described in the text.

spectra of **X** and **Y** obtained by this calculation are shown in Figure 3, panels C and D, respectively.

The spectral feature of **X** (Figure 3C) is characteristic of the ferrous NO complex of P450 (Ebel et al., 1975; O'Keeffe et al., 1978; Tsubaki et al., 1987, 1988), which exhibits EPR signals centered around $g = 2$ having rhombic symmetry and a well-resolved triplet hyperfine splitting with 2.00 mT in the absorption at $g = 2.007$ derived from the interaction of the electron spin with the nuclear spin of the nitrogen of the ligand NO. Therefore, we assigned **X** to the ferrous NO complex of P450nor. On the other hand, in the spectrum of **Y**, we observed a sharp triplet splitting of the g_z signal (2.011) with a small hyperfine constant (1.72 mT), characteristic of the ferrous NO complex of a denatured form of P450, i.e., the P420 NO complex. It is reasonable to assign **Y** to the NO complex of P420nor. Indeed, we could observe the same EPR spectrum as that in Figure 3D, when we measured at long time (>10 min) after the sample preparation (data not shown).

From the above calculation, we roughly estimated the proportion of the P450 component in the ferrous P450nor NO complex; 60% and 35% for 1 and 5 min after the sample preparation, respectively. The result shows that the NO complex of ferrous P450nor is converted into the P420nor form in the minute time domain. Compared with other usual P450s (O'Keeffe et al., 1978; Tsubaki et al., 1987), the ferrous NO complex of P450nor is extremely unstable.

Redox Potential Measurement. We measured the redox potential of P450nor by the potentiometric titration method. In Figure 4A is illustrated the visible absorption spectral change of ferric P450nor on photoreduction by proflavine sulfate and EDTA in the presence of the redox mediators under anaerobic conditions, where the electrode potential was monitored simultaneously. The difference spectral change corresponded to the reduction of ferric P450nor to its ferrous high spin form. In Figure 4B, the percent reduction of the enzyme estimated from the absorbance change was plotted against the electrode potential, showing that the potentiometric titration curve for the Fe^{3+}/Fe^{2+} couple conformed to a one-electron oxidation–reduction equilibrium with a midpoint potential ($E_{1/2}$) of −307 mV. It must be noted that

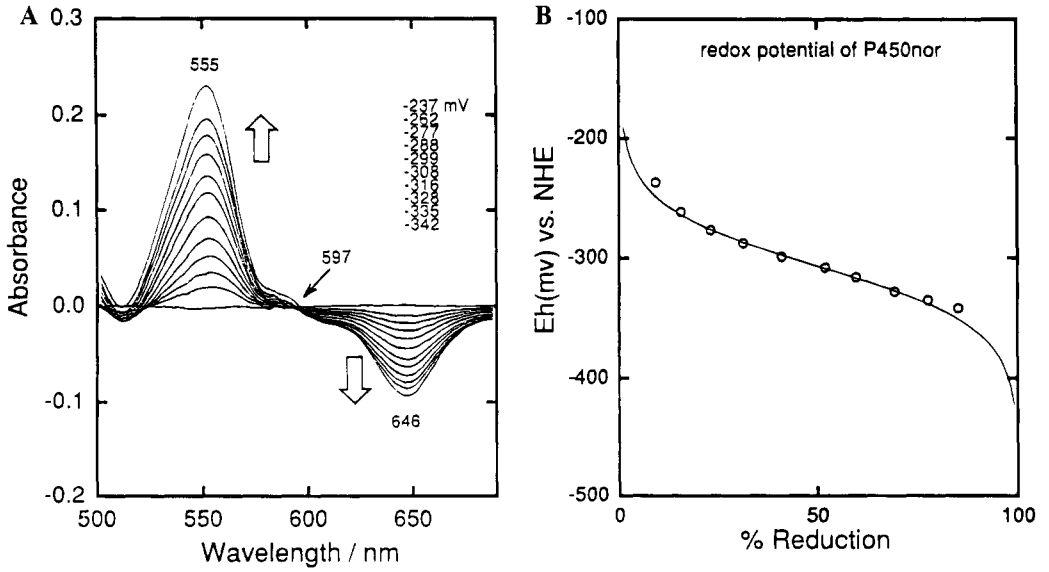

FIGURE 4: Oxidation–reduction potential measurement of P450nor. (A) The difference spectra of ferric P450nor against its ferric form was recorded during the photoreduction in the presence of proflavine sulfate and EDTA. During the reduction, electrode potentials were monitored simultaneously. (B) The degree of reduction (% Reduction) was calculated from the spectral change in (A). From the plot of the % Reduction against the electrode potential, the midpoint potential of P450nor ($E_{1/2}$) was computed to be −307 mV versus NHE.

the redox potential is much lower that those of P450cam-(+) (−140 mV) and P450cam(−) (−250 mV) (Gunsalus et al., 1974; Makino et al., 1982). The difference may reflect the structural difference in the heme environment of these enzymes and may directly relate to the difference in their functional properties, which are discussed in the Discussion section.

DISCUSSION

Immediate Configuration of Iron−Ligand Structure and Iron-Redox Property. The EPR spectra of P450nor in various spin/oxidation/ligation states are basically the same in their spectral features as those of other general P450s (Figures 1−3, Table 1). The high rhombicity ($g_x \sim 8$ and $g_y \sim 4$) in the H.S. component of the ferric resting enzyme (Figure 1) and the triplet-splitting in the central resonance ($g_z = 2.00$) in the ferrous NO complex (Figure 3C) are both characteristically seen in the EPR spectra of many P450s (Lipscomb, 1980; Ebel et al., 1975; O'Keeffe et al., 1978; Tsubaki et al., 1987, 1988). It is also notable that the hyperfine constant, A_z, in the spectrum of the ferrous NO complex (Figure 3C) is the same between P450nor and P450cam (Table 1). Likewise, the EPR spectral feature of the ferric CN^- complex is also indistinguishable between these two enzymes (Figure 2B). All these EPR results are consistent with the ligation of the Cys thiolate anion at the heme fifth site and the same configuration in the S^-−Fe−L (L: NO, CN^-) structure between P450nor and P450cam.

In the spectrum of P450nor in the ferric resting state, the *g*-values of the L.S. component are similar to those of P450cam(−), rather than those of P450cam(+) (Figure 2 and Table 1). The result is suggestive of similarity of the Fe−ligand structure of P450nor to that of P450cam(−), rather than that of P450cam(+). The difference in the heme coordination structure between P450cam(+) and P450cam-(−) has been unambiguously evaluated by X-ray crystallographic studies (Poulos et al., 1985, 1986, 1987); in P450cam(−), the sixth coordination site of its heme iron is occupied by either a water molecule or a hydroxide ion, while the site of P450cam(+) is vacant. Therefore, it is likely that either a water molecule or a hydroxide ion is present at the sixth site of the heme iron of P450nor in the L.S. component of the ferric resting state. Possibly, the distal pocket of P450nor is more hydrophilic than that of P450cam(+) but less than that of P450cam(−), in agreement with the EPR observation that the H.S. component is present in ferric resting P450nor, but its population is much less than that in P450cam(+) (Figure 1).

This result allows us to expect that the redox potential of P450nor in the Fe^{3+}/Fe^{2+} couple might fall between those of P450cam(−) (−270 mV) and P450cam(+) (−140 mV), because the H_2O ligation at the heme sixth site is considered to be one of the factors modulating the redox potential of P450cam, as was manifested in the difference in the iron coordination structures of the P450cam derivatives by the X-ray crystallography (Raag & Poulos, 1989). However, the potential of P450nor we obtained in the present work was −307 mV, which is much lower than those of P450cam-(+) and P450cam(−). Thus, another factor must be responsible for the lower redox potential. As one of the possibilities, it is likely that the heme environment of P450nor is charged either more negatively or less positively than that of P450cam, because such electrostatic interaction of the heme with its surroundings significantly controls the redox potential of the heme iron (Shiro et al., 1993). For example, replacement of Val68(E11) of myoglobin by another amino acid residue having a carboxylate group causes the redox potential to shift to a more negative value (from +57 mV for wild-type Mb to −138 mV for Mb(V68E)) (Varadarajan et al., 1989).

The extremely low redox potential is possibly related to the instability of the ferrous O_2 complex of P450nor, which is readily autoxidized to its ferric form even at −20 °C. This is possibly the reason that P450nor does not exhibit monooxygenation activity (Nakahara et al., 1993).

In the initial step of the monooxygenation reaction catalyzed by P450cam, which is a model of general P450s, the camphor-bound ferric enzyme (−140 mV) is reduced to its ferrous form with one electron transferred from NADH (∼−310 mV) through putidaredoxin reductase (flavoprotein; ∼−250 mV) and putidaredoxin (Fe−S protein; −215 mV). The resultant ferrous enzyme combines with O_2, followed by a reductive activation of the bound O_2 with one more electron and the monooxygenation reaction. In contrast, the redox potential of P450nor is comparable to that of NADH, but the electrons are not transferred from NADH to the ferric resting enzyme. This fact may relate to no other redox cofactors such as flavin− and Fe−S proteins. However, upon the NO binding to the ferric P450nor, the electrons are directly transferred from NADH to the enzyme to initiate the NO reduction. Most probably, the NO binding causes the protein conformation to change into one which can accept electrons from NADH.

Distal Pocket Structure. In the EPR spectral features, the most prominent difference in the *g*-value was seen in the ferric metyrapone complex, where the magnitude in the difference between P450nor and P450cam is 0.07−0.09 (Table 1). On the basis of their *g*-values, we estimated the ligand field parameters, V/λ, Δ/λ and V/Δ, to be 3.55, 4.74, and 0.75, respectively, and compared them with those of P450cam (4.53, 5.20, and 0.87), where V, Δ, and λ represent rhombicity, tetragonality, and the spin-orbital coupling constant, respectively (Taylor, 1977). All these values decrease on going from P450cam to P450nor, indicating an increase in symmetry around the iron−ligand structure. However, in the case of the enzyme combined with a small molecule such as NO, CN^-, or H_2O, the immediate configuration of the Fe−ligand structure is essentially the same between P450nor and P450cam, as was manifested in their EPR spectral features. This is not the case for the metyrapone complex, suggesting that another specific factor may influence the structural and/or electronic state in the Fe−ligand moiety of the metyrapone complex.

The crystallographic data of the metyrapone complex of ferric P450cam (Poulos & Howard, 1987) showed that the nitrogen atom of one pyridine ring of metyrapone coordinates to the heme iron at the iron sixth site. In spite of binding such a large molecule at the heme sixth site, the structural difference in the heme distal pocket is surprisingly small between the metyrapone-bound and -unbound P450cam, because another pyridine ring fits well to the camphor binding site. The hydroxyl group of Tyr96 in P450cam is in position to donate a hydrogen bond to the nitrogen atom of another pyridine ring of metyrapone, which is very similar

to the camphor oxygen and Tyr96 hydrogen bond in P450cam(+).

On the other hand, the catalytic reaction of P450nor allows us to suppose that this enzyme does not have a binding site for organic substrates in its heme distal pocket. Further, in alignment of the primary structure of P450nor with that of P450cam, the Tyr96 is replaced with Ala80 (Kizawa et al., 1991), showing no interaction site for the metyrapone pyridine ring. Thus, it seems reasonable that the metyrapone ligand could interact with the protein part in the heme distal pocket of P450nor in a different manner from that in P450cam. It is likely that no hydrogen bonding interaction of one pyridine ring with the surroundings may cause the metyrapone to bind the heme iron in a different manner, probably resulting in higher symmetry around the iron. In other words, the difference in the EPR spectral features between the metyrapone complexes of P450nor and P450cam reflects their structural difference in the heme distal pocket.

Support for the different structure at the heme distal side was recently provided from our kinetic and thermodynamic study of the CO binding to P450nor (Shiro et al., 1994). The CO association rate constant increases in the order of P450cam(+), P450nor, and P450cam(−), suggesting that the ligand binding pocket is opened more widely for P450nor than for P450cam(+) but more narrowly than for P450(−). The activation entropy change in P450nor, $\Delta S°$, upon the CO binding, which is much smaller than that of P450cam(±), can be accounted for in terms of no substrate binding site in P450nor. The difference in the heme distal side possibly relates to the unique function of P450nor.

Relation to Reaction Mechanism. It is interesting to compare the molecular properties of P450nor such as EPR and redox properties with those of the bacterium NOR from *P. stutzeri*, cytochrome *bc* complex (Kastrau et al., 1994; Zumft, 1993). The redox potentials of cytochrome *b* and *c* components in the Fe^{3+}/Fe^{2+} couple were measured to be +322 and +280 mV, respectively. Judging from the values, it is true that the electron is transferred from cytochromes *c* to *b* and that cytochrome b provides the reaction center in the NO reduction reaction. The EPR and absorption spectral data of cytochrome *b* support that the heme iron is a five-coordination complex having a nitrogenous ligand at its fifth site. All these observations for the cytochrome *bc* complex, NOR of *P. stutzeri*, are sharply contrasted to those for P450nor: the $Fe-S^-$ structure and the negative value (−307 mV) of $E_{1/2}$ in the Fe^{3+}/Fe^{2+} couple. Therefore, we can reasonably suggest that the reaction mechanism of the NO reduction is not necessarily similar between P450nor and the cytochrome *bc* complex.

The NO reduction mechanism catalyzed by the cytochrome *bc* complex remains unclear and controversial. One of the most possible mechanisms was proposed by Hollocher et al. (Dermastia et al., 1991; Turk & Hollocher, 1992), where NO^- produced in the one-electron reduction of NO by NOR is nonenzymatically dimerized to yield N_2O. However, some investigators have criticized this mechanism, because the one-electron reduction of NO by cytochrome *b* having a highly positive redox potential (+322 mV) is thermodynamically difficult (Ye et al., 1994).

In contrast, P450nor having an extremely negative value of its redox potential (−307 mV) has the possibility of reductive activation of the NO ligand at the heme sixth site. Most recently, we proposed a reaction mechanism of the NO reduction to N_2O catalyzed by P450nor on the basis of the spectroscopic and kinetic results of its ferric NO complex with NADH (Shiro et al., 1995). In that study, we spectrophotometrically found a characteristic intermediate during the catalytic cycle and assigned it as a two-electron reduced species of the ferric P405nor NO complex; i.e., $Fe^{3+}NO + 2e^- \rightarrow (Fe^{3+}NO)^{2-}$. Subsequently, the Fe-bound NO in the intermediate species reacts with another free NO on the iron center to yield N_2O. Although the characterization of the intermediate has not been completed yet, it is likely that the heme iron of P450nor with the low redox potential can support its formation in the reaction of its ferric NO complex with NADH.

ACKNOWLEDGMENT

We greatly thank Dr. H. Hori (Osaka University) for his valuable suggestions and discussion.

REFERENCES

Carr, G. J., & Ferguson, S. J. (1990) *Biochem. J. 269*, 423−429.
Carr, G. J., Page, M. D., & Ferguson, S. J. (1989) *Eur. J. Biochem. 179*, 683−692.
Dawson, J. H., Andersson, L. A., & Sono, M. (1982) *J. Biol. Chem. 257*, 3606−3617.
Dermastia, M., Turk, T., & Hollocher, T. C. (1991) *J. Biol. Chem. 266*, 10899−10905.
Ebel, R. E., O'Keeffe, D. H., & Peterson, J. A. (1975) *FEBS Lett. 55*, 198−201.
Goretski, J., & Hollocher, T. C. (1990) *J. Biol. Chem. 265*, 889−895.
Gunsalus, I. C., Meeks, J. R., Lipscomb, J. D., Debrunner, P., & Munck, E. (1974) in *Molecular Mechanisms of Oxygen Activation* (Hayaishi, O., Ed.) Chapter 14, pp 559−613, Academic Press, New York.
Heiss, B., Frunzke, K., & Zumft, W. G. (1989) *J. Bacterol. 171*, 3288−3297.
Hoglen, J., & Hollocher, T. C. (1989) *J. Biol. Chem. 264*, 7556−7563.
Kastrau, D. H. W., Heiss, B., Kroneck, P. M. H., & Zumft, W. G. (1994) *Eur. J. Biochem. 222*, 293−303.
Kizawa, H., Tomura, D., Oda, M., Fukumizu, A., Hoshino, T., Gotoh, O., Yasui, T., & Shoun, H. (1991) *J. Biol. Chem. 266*, 10632−10637.
Lipscomb, J. D. (1980) *Biochemistry 19*, 3590−3599.
Makino, R., Iizuka, T., Sakaguchi, K., & Ishimura, Y. (1982) in *Oxygenase and Oxygen Metabolism* (Nozaki, M., Yamamoto, S., Ishimura, Y., Coon, M. J., Ernster, L., & Estabrook, R. W., Eds.) pp 467−477, Academic Press, New York.
Nakahara, K., Tanimoto, T., Hatano, K., Usuda, K., & Shoun, H. (1993) *J. Biol. Chem. 268*, 8350−8355.
Nakahara, K., Shoun, H., Adachi, S., Iizuka, T., & Shiro, Y. (1994) *J. Mol. Biol. 239*, 158−159.
Obika, K., Tomura, D., Fukumizu, A., & Shoun, H. (1993) *Biochem. Biophys. Res. Commun. 196*, 1255−1260.
O'Keeffe, D. H., Ebel, R. E., & Peterson, J. A. (1978) *J. Biol. Chem. 253*, 3509−3516.
Peterson, J. A., Ullrich, V., & Hildebrandt, A. G. (1971) *Arch. Biochem. Biophys. 145*, 531−542.
Poulos, T. L., & Howard, A. J. (1987) *Biochemistry 26*, 8165−8174.
Poulos, T. L., Finzel, B. C., Gunsalus, I. C., Wagner, G. C., & Kraut, J. (1985) *J. Biol. Chem. 260*, 16122−16130.
Poulos, T. L., Finzel, B. C., & Howard, A. J. (1986) *Biochemistry 25*, 5314−5322.
Poulos, T. L., Finzel, B. C., & Howard, A. J. (1987) *J. Mol. Biol. 195*, 687−700.
Raag, R., & Poulos, T. L. (1989) *Biochemistry 28*, 917−922.
Shiro, Y., Iwata, T., Makino, R., Fujii, M., Isogai, Y., & Iizuka, T. (1993) *J. Biol. Chem. 268*, 19983−19990.
Shiro, Y., Kato, M., Iizuka, T., Nakahara, K., & Shoun, H. (1994) *Biochemistry 33*, 8673−8677.

Shiro, Y., Fujii, M., Iizuka, T., Adachi, S., Tsukamoto, K., Nakahara, K., & Shoun, H. (1995) *J. Biol. Chem.*, 1617−1623.
Shoun, H., & Tanimoto, T. (1991) *J. Biol. Chem. 266*, 11078−11082.
Shoun, H., Sudo, Y., Seto, Y., & Beppu, T. (1983) *J. Biochem. 94*, 1219−1229.
Shoun, H., Suyama, W., & Yasui, T. (1989) *FEBS Lett. 244*, 11−14.
Taylor, C. P. S. (1977) *Biochim. Biophys. Acta 491*, 137−149.
Tsubaki, M., Hiwatashi, A., Ichikawa, Y., & Hori, H. (1987) *Biochemistry 26*, 4527−4534.
Tsubaki, M., Hiwatashi, A., Ichikawa, Y., Fujimoto, Y., Ikekawa, N., & Hori, H. (1988) *Biochemistry 27*, 4856−4862.
Turk, T., & Hollocher, T. C. (1992) *Biochem. Biophys. Res. Commun. 183*, 983−988.
Varadarajan, R., Zewert, T. E., Gray, H. B., & Boxer, S. G., (1989) *Science 243*, 69−72.
Ye, R. W., Averill, B. A., & Tiedje, J. M. (1994) *Appl. Environ. Microbiol. 60*, 1053−1058.
Zumft, W. G. (1993) *Arch. Microbiol. 160*, 253−264.

BI950110W